

# Cost-Effective Federated Learning in Mobile Edge Networks

Bing Luo, *Member, IEEE*, Xiang Li, *Student Member, IEEE*, Shiqiang Wang, *Member, IEEE*, Jianwei Huang, *Fellow, IEEE*, Leandros Tassiulas, *Fellow, IEEE*

**Abstract**—Federated learning (FL) is a distributed learning paradigm that enables a large number of mobile devices to collaboratively learn a model under the coordination of a central server without sharing their raw data. Despite its practical efficiency and effectiveness, the iterative on-device learning process (e.g., local computations and global communications with the server) incurs a considerable cost in terms of learning time and energy consumption, which depends crucially on the number of selected clients and the number of local iterations in each training round. In this paper, we analyze how to design adaptive FL in mobile edge networks that optimally chooses these essential control variables to minimize the total cost while ensuring convergence. We establish the analytical relationship between the total cost and the control variables with the convergence upper bound. To efficiently solve the cost minimization problem, we develop a low-cost sampling-based algorithm to learn the convergence related unknown parameters. We derive important solution properties that effectively identify the design principles for different optimization metrics. Practically, we evaluate our theoretical results both in a simulated environment and on a hardware prototype. Experimental evidence verifies our derived properties and demonstrates that our proposed solution achieves near-optimal performance for different optimization metrics for various datasets and heterogeneous system and statistical settings.

**Index Terms**—Federated learning, mobile edge networks, cost analysis, scheduling, optimization algorithm.

## I. INTRODUCTION

With the rapid advancement of Internet of Things (IoT) and social networking applications, there is an exponential increase of data generated at network edge devices, such as smartphones, IoT devices, and sensors [2]. These valuable

data provide highly useful information for the prediction, classification, and other intelligent applications, which can improve our daily lives [3]. To analyze and exploit the large amount of data, standard machine learning (ML) techniques normally require collecting the training data in a central server. However, such centralized data collection and training can be quite challenging to perform due to limited communication bandwidth and data privacy concerns [4], [5].

To tackle this challenge, *Federated learning (FL)* has emerged as an attractive distributed learning paradigm, which enables many clients<sup>1</sup> to collaboratively train a model under the coordination of a central server, while keeping the training data decentralized and private [6], [7]. In FL settings, the training data are in general massively distributed over a large number of clients, and the communications between the server and clients are typically operated at lower rates compared to datacenter settings. These unique features necessitate FL algorithms to perform *multiple local iterations* in parallel on *a fraction of randomly sampled clients* and then aggregate the resulting model update via the central server periodically [7].<sup>2</sup>

FL has demonstrated its effectiveness in various *statistically heterogeneous* settings, e.g., unbalanced and non-independent and identically distributed (non-i.i.d.) data [9]–[12]. Nevertheless, an efficient deployment of FL in mobile edge networks also needs to consider *system heterogeneity*. This is because in mobile edge environment, the system bandwidth is limited and shared by all connected mobile devices with potential mutual interference. Moreover, the selected devices may have different computational capabilities and dynamic wireless channel conditions due to mobility and channel fading, thus an efficient scheduling strategy in FL should adapt to system heterogeneity.

Because model training and information transmission for on-device FL can be both time and energy consuming, it is necessary and important to analyze the *cost* that is incurred for completing a given FL task. In general, the cost of FL includes multiple components such as learning time and energy consumption [13]. The importance of different cost components depends on the characteristics of FL systems and applications. For example, in a solar-based sensor network, energy consumption is the major concern for the sensors

<sup>1</sup>Depending on the type of clients, FL can be categorized into cross-device FL and cross-silo FL (clients are companies or organizations, etc.) [6]. This paper focuses on the former and we use “device” and “client” interchangeably.

<sup>2</sup>Model compression is also an effective approach for improving FL communication efficiency. While orthogonal to the focus of this work, standard compression approaches such as sketched or random masking and model pruning [6], [8] can be used together to further reduce the cost.

Bing Luo is with Shenzhen Institute of Artificial Intelligence and Robotics for Society, The Chinese University of Hong Kong, Shenzhen, China, and the Department of Electrical Engineering and Institute for Network Science, Yale University, USA. (e-mail: luobing@cuhk.edu.cn)

Xiang Li and Jianwei Huang (corresponding author) are with the School of Science and Engineering, The Chinese University of Hong Kong, Shenzhen, China, and the Shenzhen Institute of Artificial Intelligence and Robotics for Society, Shenzhen, China. (e-mail:lixiang@cuhk.edu.cn; jianwei-huang@cuhk.edu.cn)

Shiqiang Wang is with IBM T. J. Watson Research Center, Yorktown Heights, NY, USA. (e-mail: shiqiang.wang@ieee.org)

Leandros Tassiulas is with the Department of Electrical Engineering and Institute for Network Science, Yale University, USA. (e-mail: leandros.tassiulas@yale.edu)

The research of Bing Luo was supported by the AIRS-Yale Joint Postdoctoral Fellowship. The research of Xiang Li and Jianwei Huang was supported by the Shenzhen Science and Technology Program (JCYJ20210324120011032), Shenzhen Institute of Artificial Intelligence and Robotics for Society, and the Presidential Fund from the Chinese University of Hong Kong, Shenzhen. The research of Leandros Tassiulas was supported by the NSF CNS-2112562 AI Institute for Edge Computing Leveraging Next Generation Networks (Athena) and the ONR N00014-19-1-2566. This paper was presented in part at the IEEE INFOCOM, Virtual Conference, 2021 [1].

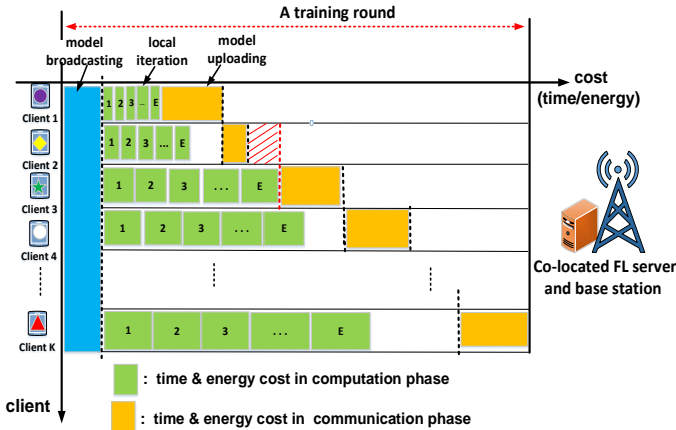


Fig. 1. A heterogeneous federated learning training round in mobile network, where  $K$  sampled clients performs  $E$  steps of local iteration and communicates with the BS with time-sharing.

to participate in FL tasks, whereas in a multi-agent search-and-rescue task where the goal is to collaboratively learn an unknown map, achieving timely result would be the first priority. Therefore, a cost-effective FL design needs to *jointly optimize various cost components* (e.g., learning time and energy consumption) *for different preferences*.

A way of optimizing the cost is to adapt control variables in the FL process to achieve a properly defined objective. For example, some existing works have considered the adaptation of communication interval (i.e., the number of local iterations between two global aggregation rounds) for communication-efficient FL with convergence guarantees [14], [15]. However, a limitation in these works is that they only adapt a single control variable (i.e., communication interval) in the FL process and ignore other essential aspects, such as the number of participating clients in each round, which can have a significant impact on the energy consumption.

In this paper, we consider a *multivariate* control problem for wireless FL with convergence guarantees. To minimize the expected cost, we develop an algorithm that adapts these control variables in the FL process to achieve our goal. Compared to the univariate setting in existing works, our *multivariate* control problem is much more challenging due to the following reasons: 1) The choices of control variables are tightly coupled due to system and statistical heterogeneity. 2) The relationship between the control variables and the learning convergence rate has only been captured by an upper bound with unknown coefficients in the literature. 3) Our cost objective includes multiple components (e.g., time and energy) which can have different importance depending on the application scenario, whereas existing works often consider a single optimization objective, e.g., minimizing the communication overhead. In light of the above discussion, we state the key contributions of this work as follows:

- *Cost-effective Wireless FL Design*: This work, for the first time, analyzes how to design adaptive FL that optimally chooses the number of participating clients ( $K$ ) and the number of local iterations ( $E$ ) to minimize the *total*

cost in mobile edge networks. Considering the wireless bandwidth limitation and interference, we propose a new scheduling scheme, as illustrated in Fig. 1, which characterizes both computation and communication heterogeneity.

- *Optimization Algorithm*: We establish the analytical relationship between the total cost, control variables, heterogeneous system parameters, and convergence upper bound, based on which we formulate and analyze the optimization problem for total cost minimization. When facing the challenging issue of estimating the unknown coefficients in the convergence bound, we develop an effective sampling-based algorithm to learn these parameters with a small estimation overhead.
- *Theoretical Properties*: We obtain important analytical properties that effectively identify the design principles of  $K$  and  $E$  for different optimization metrics and heterogeneous system parameters. Notably, the choice of  $K$  leads to an interesting trade-off between learning time reduction and energy saving, with a relatively large  $K$  favoring the former while  $K = 1$  always benefiting the latter. In contrast, the total cost, no matter emphasizing learning time or energy consumption, always first decreases and then increases in  $E$ . We also show how heterogeneous system parameters in terms of computation and communication affect the optimal  $K$  and  $E$ .
- *Simulation and Experimentation*: We evaluate our theoretical results with real and synthetic heterogeneous datasets, both in a simulated wireless cellular network and on a WiFi-based hardware prototype. Experimental results demonstrate that our proposed optimization algorithm provides near-optimal solution for different optimization metrics, and verify our theoretical findings for design principles and solution properties.

The rest of the paper is organized as follows. We first present the related work in Section II. Then, we present the system model and problem formulation in Section III. In Section IV, we analyze the cost minimization problem and present an algorithm to solve it. We provide theoretical analysis on the solution properties in Section V. Experimentation results are given in Section VI and the conclusion is presented in Section VII.

## II. RELATED WORK

FL was first proposed in [7], which demonstrated FL's effectiveness of collaboratively learning a model without collecting users' data. The de facto FL algorithm is federated averaging (FedAvg), which performs multiple local iterations in parallel on a subset of devices in each round. A system-level FL framework [9] demonstrates the empirical success of FedAvg in mobile devices. Recently, a convergence bound of FedAvg was established in [10]. Other related distributed optimization algorithms are mostly analyzed for homogeneous and i.i.d. datasets (e.g., [16]–[18]) and full client participation (e.g., [19], [20]), which do not capture the essence of on-device FL. Some extensions of FedAvg considered aspects such as adding a proximal term [21], using gradient descent

TABLE I  
SUMMARY OF RELATED WORK FOR FL COST MINIMIZATION WITH CONTROL PARAMETERS

reference	optimization goal		control parameters			
	training time	energy consumption	local iteration number	sampled client number	mobile clients scheduling	resource allocation (CPU/power/bandwidth)
[13]	✓	✓			✓	✓
[14]	✓	✓	✓			
[15]	✓		✓			
[27]	✓				✓	✓
[28]	✓			✓		
[29]	✓			✓	✓	
[30]	✓				✓	✓
[31]	✓				✓	✓
[33]	✓				✓	
[34]		✓			✓	✓
[35]		✓			✓	✓
[36]		✓			✓	✓
[37]		✓			✓	✓
[38]	✓		✓			
[39]	✓		✓			
[41]	✓		✓	✓		
<b>this work</b>	✓	✓	✓	✓	✓	

acceleration [22], variance reduction (e.g., [23], [24]), or fine tuning hyper-parameters [25], [26]. While novel insights are provided in these works, they did not consider optimization for cost/resource efficiency.

Literature in FL cost optimization mainly focused on learning time and on-device energy consumption in mobile edge networks. The optimization of learning time was studied in [8], [27]–[33], and joint optimization for learning time and energy consumption was considered in [34]–[37]. These works considered resource (e.g., transmission power, communication bandwidth, and CPU frequency) allocation (e.g., [27], [28], [34]–[37]), cost-aware client selection (e.g., [29], [30]), client scheduling (e.g., [31]–[33]), and model pruning [8] for *pre-specified* (i.e., non-optimized) design parameters ( $K$  and  $E$  in our case) of the FL algorithm.

The optimization of a single design parameter  $E$  was studied in [14], [15], [38]–[40], most of which assume full client participation and can be infeasible for large-scale on-device FL. A very recent work in [41] considered the optimization of both  $E$  and client selection for additive per-client costs. However, the cost of learning time in our problem is non-additive on a per-client basis, since different clients perform local model updates in parallel. In addition, the convergence bound used in [41] (also [13]) is for a primal-dual optimization algorithm, which is different from the commonly used FedAvg algorithm. The challenge in optimizing both  $K$  and  $E$  for cost minimization of FedAvg, which also distinguishes our work from the above, is the need to *analytically connect the total cost with the control variables as well as with the convergence rate*. The comparison of our work with the above related works is illustrated in Table I, where we note that our optimization design is orthogonal to most works on resource allocation in the last column in Table I and can be used together with those techniques to further reduce the cost.

In addition, most existing work on FL are based on simulations, whereas we implement our algorithm in an actual hardware prototype with resource-constrained devices.

### III. SYSTEM MODEL AND PROBLEM FORMULATION

We start by summarizing the basics of FL and its de facto algorithm FedAvg. Then, we introduce the scheduling strategy when applying FL in mobile edge networks with system heterogeneity. Finally, we present the cost optimization problem for FL tasks. We summarize all key notations in this paper in Table II.

#### A. Federated Learning

Consider a scenario with a large number of mobile clients that have data for training a machine learning model. Due to data privacy concern, it is not desirable for clients to disclose and send their raw data to a high-performance data center. FL is a decentralized learning framework that aims to resolve this problem. Mathematically, FL is the following distributed optimization problem:

$$\min_{\mathbf{w}} F(\mathbf{w}) := \sum_{k=1}^N p_k F_k(\mathbf{w}) \quad (1)$$

where the objective  $F(\mathbf{w})$  is also known as the global loss function,  $\mathbf{w}$  is the model parameter vector,  $N$  is the total number of devices, and  $p_k > 0$  is the weight of the  $k$ -th device such that  $\sum_{k=1}^N p_k = 1$ . Suppose the  $k$ -th device has  $n_k$  training data samples  $(\mathbf{x}_{k,1}, \dots, \mathbf{x}_{k,n_k})$ , and the total number of training data samples across  $N$  devices is  $n := \sum_{k=1}^N n_k$ , then we have  $p_k = \frac{n_k}{n}$ . The local loss function of client  $k$  is

$$F_k(\mathbf{w}) := \frac{1}{n_k} \sum_{j=1}^{n_k} f(\mathbf{w}; \mathbf{x}_{k,j}), \quad (2)$$

where  $f(\cdot)$  represents a per-sample loss function, e.g., mean square error or cross entropy applied to the output of a model with parameter  $\mathbf{w}$  and input data sample  $\mathbf{x}_{k,j}$  [14].

FedAvg (Algorithm 1) was proposed in [7] to solve (1). In each *round*  $r$ , a subset of randomly selected clients  $\mathcal{K}^r$  run  $E$  steps<sup>3</sup> of stochastic gradient decent (SGD) on (2) in

<sup>3</sup> $E$  is originally defined as epochs of SGD in [7]. In this paper we denote  $E$  as the number of local iterations for theoretical analysis.

TABLE II  
SUMMARY OF ALL KEY NOTATIONS

$F(\mathbf{w})$	Global loss function
$F_k(\mathbf{w})$	Local loss function
$\mathbf{w}^*$	Optimal model parameter that minimizes $F(\mathbf{w})$
$\mathbf{w}_R$	Final model parameter after $R$ rounds
$\epsilon$	Desired precision with $\mathbb{E}[F(\mathbf{w}_R)] - F^* \leq \epsilon$
$R$	Final round number for achieving $\epsilon$
$r$	Round number index
$\mathcal{K}^r$	Randomly selected clients in round $r$
$K$	Number of selected clients with $K :=  \mathcal{K}^r $
$E$	Number of local iteration steps
$T^r$	Round time in round $r$
$e^r$	Energy consumption in round $r$
$t_{k,p}$	Computation time of client $k$ for one iteration
$e_{k,p}$	Computation energy of client $k$ for one iteration
$t_{k,m}^r$	Communication time of client $k$ in round $r$
$e_{k,m}^r$	Communication energy of client $k$ in round $r$
$\bar{t}_{k,m}^r$	Expected $t_{k,m}^r$ in $R$ rounds
$\bar{e}_{k,m}^r$	Expected $e_{k,m}^r$ in $R$ rounds
$t_p$	Expected per-device per-iteration computation time
$e_p$	Expected per-device per-iteration computation energy
$t_m$	Expected per-device per-round communication time
$e_m$	Expected per-device per-round communication energy
$T_{\text{tot}}$	Total learning time after $R$ rounds
$e_{\text{tot}}$	Total energy consumption after $R$ rounds
$T_k^r$	Time after scheduling client $k$ in round $r$
$C_{\text{tot}}$	Balanced total cost
$\gamma$	Normalized price factor
$A_0, B_0$	Unknown constants in convergence bound
$F_a, F_b$	Pre-defined global loss for estimation $A_0, B_0$
$R_a, R_b$	Pre-defined round number for estimation $A_0, B_0$

### Algorithm 1: Federated Learning Algorithm

**Input:**  $K, E$ , precision  $\epsilon$ , initial model  $\mathbf{w}_0$ , initial round index  $r = 0$

**Output:** Final model parameter  $\mathbf{w}_R$

```

1 while  $r \leq R$  do
2   Server randomly selects a subset of clients  $\mathcal{K}^r$  and
   broadcast the current global model parameter  $\mathbf{w}_r$  to the
   selected clients; // Communication
3   Each selected client  $k \in \mathcal{K}^r$  in parallel updates  $\mathbf{w}_r$  by
   running  $E$  steps of SGD on (2) to compute a new
   model  $\mathbf{w}_r^{(k)}$ ; // Computation
4   Each selected client  $k \in \mathcal{K}^r$  sends back the updated
   model  $\mathbf{w}_r^{(k)}$  to the server; // Communication
5   Server computes the new global model parameter
    $\mathbf{w}_{r+1} \leftarrow \frac{\sum_{k \in \mathcal{K}^r} p_k \mathbf{w}_r^{(k)}}{\sum_{k \in \mathcal{K}^r} p_k}$ ; // Aggregation
6    $r \leftarrow r + 1$ ;

```

parallel, where  $\mathcal{K}^r \subseteq \{1, 2, \dots, N\}$ . Then, the updated model parameters of these  $|\mathcal{K}^r|$  clients are sent to and aggregated by the server. This process repeats for many rounds until the global loss converges.

FL has demonstrated its effectiveness in tackling with statistical heterogeneity, e.g., unbalanced and non-i.i.d. data distribution. Meanwhile, applying it in practical mobile edge networks also needs to address clients' computational and communication heterogeneity. Therefore, an efficient FL design requires *joint consideration of statistical and system heterogeneity*.

## B. Deploying Federated Learning in Mobile Edge Networks

In mobile edge networks, due to system bandwidth limitation and wireless interference, participating clients are usually scheduled in a time-sharing (TS) [13], [34] or frequency-sharing (FS) [27], [30], [36] protocols.<sup>4</sup> However, the selected heterogeneous clients may have diverse communication and computation capabilities, which results in different per-round training time under different scheduling strategies, especially for clients with dynamic wireless channels. This is because the per-round time depends on the slowest client (known as straggler), as the server needs to collect all updates from the sampled clients before performing global aggregation.

In this paper, as shown in Fig. 1, we propose a new TS based FL model which works efficiently with heterogeneous computation and communication time. We note that the empirical results in Section VI demonstrate that our proposed TS is superior to existing FS schemes in [42]–[44]. The main reason is that, in those FS schemes, the frequency allocation for the sampled clients in each round is *static*, which causes a waste in bandwidth resources. This is because, due to computational heterogeneity, clients who complete computation early can be allocated with more bandwidth for transmission before the next client completing computation, instead of always sharing the entire bandwidth static with other slower clients. In the following, we first describe our system model and then present the proposed TS protocol.

1) **System Model:** Similar to existing works [7], [10], [21], we sample  $K$  clients in each round  $r$  (i.e.,  $K := |\mathcal{K}^r|, 1 \leq K \leq N$ ), where the sampling is uniform at random (without replacement) out of all  $N$  clients. Similar to existing studies on wireless FL (e.g., [27], [30], [36]), we assume that a particular device has the same computation cost (time and energy) over multiple rounds, whereas the communication cost varies between rounds due to wireless dynamics. We do not consider the server's downlink cost for model broadcasting and model aggregation, as we mainly focus on the performance bottleneck of the battery-constrained edge devices.

2) **Proposed Time-sharing Protocol:** Consider a general round  $r$ , where the server (co-located with the base station) first broadcasts the current global model to the randomly selected  $\mathcal{K}^r$  clients. Then, each of the selected clients performs  $E$  steps of local iterations *in parallel*, where we denote  $t_{k,p}$  as the computation time for client  $k$  to perform one local iteration. In the communication phase, however, the selected clients *sequentially* upload their model to the server in different time slots, where we denote  $t_{k,m}^r$  as the communication time

<sup>4</sup>We consider cellular network based one-hop communication between the server and the clients, since its topology is well-aligned with that in mainstream FL community. For FL in a decentralized topology, e.g., in wireless ad-hoc networks, the communications could be multi-hop, which is beyond our focus in this work. Although leveraging analog aggregation techniques in wireless communications [42]–[44] can increase the communication efficiency, it may require stringent synchronization and additional superposition code design.

for client  $k$  to upload the model parameter in round  $r$ .<sup>5</sup>

Due to the difference between  $t_{k,p}$  and  $t_{k,m}^r$  among the selected  $K$  clients in  $\mathcal{K}^r$ , the time of round  $r$  depends on the *scheduling order* of the  $K$  clients. We present the optimal TS scheduling with the following theorem, which achieves the minimum time for a particular round  $r$  with the selected clients  $\mathcal{K}^r$ . We note that the proposed scheduling scheme mainly considers the total learning time for the sampled clients rather than their energy consumption. This is because the total energy consumption is the sum of all sampled clients' energy cost, which is independent of the scheduling order of the  $K$  clients.

**Theorem 1. (Optimal time-sharing scheduling)** *For any sampled clients set  $\mathcal{K}^r$  in round  $r$ , without loss of generality, we assume that  $\mathcal{K}^r$  is ordered based on  $\{t_{k,p} : \forall k \in \mathcal{K}^r\}$ , such that  $t_{1,p} \leq \dots \leq t_{k,p} \leq \dots \leq t_{K,p}$ . Then, sequentially scheduling the ordered  $K$  clients yields the minimum time of round  $r$ , compared to any other scheduling sequence. Under this scheduling sequence, denoting  $T_k^r$  as the time after scheduling client  $k$ , we have*

$$T_k^r = \max \{t_{k,p}E, T_{k-1}^r\} + t_{k,m}^r, \quad k \in \{1, \dots, K\}, \quad (3)$$

where  $T_K^r$  is the entire time of round  $r$  after scheduling all  $K$  clients, and we define  $T_0^r := 0$  and  $T^r := T_K^r$  for convenience.

We give the proof in Appendix A. Compared to existing TS scheduling strategy in [13] where communication from the clients to the server will not begin until all sampled clients complete local iterations, the scheduling policy specified in Theorem 1 enables each client to upload its result to the server as soon as it finishes the computation when the wireless channel is available, which potentially reduces system waiting time and thus the round time  $T^r$ . The *max* function in (3) characterizes whether the channel is vacant when a certain client completes its local iteration, e.g., the red shadow time slots in Fig. 1.

### C. Cost Analysis of Federated Learning in Mobile Edge Networks

Despite the effectiveness and efficiency of FL, practitioners need to take into account the cost of completing FL tasks. The total cost of FL, according to Fig. 1, involves *learning time* and *energy consumption*, both of which are consumed during local computation and global communication in each round.

1) **Time Cost:** Based on the optimal TS scheduling in Theorem 1, the per-round time after scheduling the selected  $K$  clients is  $T^r$ , which depends on the number of sampled clients  $K$  and the number of location computation steps  $E$ . The total learning time  $T_{\text{tot}}$  after  $R$  rounds is

$$T_{\text{tot}}(K, E, R) = \sum_{r=1}^R T^r. \quad (4)$$

<sup>5</sup>We note that  $t_{k,m}^r$  can be calculated by  $t_{k,m}^r = \Omega/B \log \left(1 + \frac{p_k \bar{h}_k^r}{N_0}\right)$ , where  $\Omega$  is the size of model parameter,  $B$  is the bandwidth,  $p_k$  is the transmission power (we do not consider power control in this work, though it can be incorporated in future work),  $\bar{h}_k^r$  is the average channel gain of the client  $k$  during the FL training time in round  $r$  and  $N_0$  is the white noise power.

2) **Energy Cost:** Similar to the notation for time cost, by denoting  $e_k$  as the per-round energy consumption for client  $k$  to complete the computation and communication, we have

$$e_k^r = e_{k,p}E + e_{k,m}^r, \quad (5)$$

where  $e_{k,p}$  is the computation energy for client  $k$  to perform one step local iteration in each round, and  $e_{k,m}^r$  is client  $k$ 's communication energy in round  $r$  due to wireless dynamics.

Unlike the per-round time cost, the energy cost  $e^r$  in each round  $r$  depends on the *sum* energy consumption of the selected  $K$  clients. Therefore, the total energy cost  $e_{\text{tot}}$  after  $R$  rounds can be expressed as

$$e_{\text{tot}}(K, E, R) = \sum_{r=1}^R \sum_{k \in \mathcal{K}^r} e_k^r. \quad (6)$$

### D. Problem Formulation

Considering the difference of the two cost metrics, the optimal solutions of  $K$ ,  $E$  and  $R$  generally do not achieve the common goal for minimizing both  $T_{\text{tot}}$  and  $e_{\text{tot}}$ . To strike the balance between learning time and energy consumption, we introduce a weight  $\gamma \in [0, 1]$  and optimize the balanced cost function in the following form:

$$C_{\text{tot}}(K, E, R) = \gamma e_{\text{tot}}(K, E, R) + (1 - \gamma) T_{\text{tot}}(K, E, R), \quad (7)$$

where  $1 - \gamma$  and  $\gamma$  can be interpreted as the *normalized price* of the two costs, i.e., how much monetary cost for one unit of time and one unit of energy, respectively. The value of  $\gamma$  can be adjusted for different preferences. For example, we can set  $\gamma = 0$  when all clients are plugged in and energy consumption is not a major concern, whereas  $\gamma = 1$  when devices are solar-based sensors where saving the devices' energy is the priority.

Our goal is to minimize the expected total cost while ensuring convergence, which translates into this problem:

$$\begin{aligned} \mathbf{P1}: \quad & \min_{E, K, R} \quad \mathbb{E}[C_{\text{tot}}(E, K, R)] \\ & \text{s.t.} \quad \mathbb{E}[F(\mathbf{w}_R)] - F^* \leq \epsilon, \\ & \quad K, E, R \in \mathbb{Z}^+, \text{ and } 1 \leq K \leq N. \end{aligned} \quad (8)$$

where  $\mathbb{E}[F(\mathbf{w}_R)]$  is the expected loss after  $R$  rounds,  $F^*$  is the (true and unknown) minimum value of  $F$ , and  $\epsilon$  is the desired precision. We note that the expectation in Problem **P1** takes over three source of randomness, where the first two randomness come from the client sampling and data sampling in SGD in each round, and the third randomness comes from the varying communication cost in each round due to dynamic wireless channel conditions.

Solving Problem **P1** is challenging in two aspects. First, it is difficult to find an *exact analytical expression* to relate  $K$ ,  $E$  and  $R$  with  $C_{\text{tot}}$ , especially due to the *maximum* function in  $T_{\text{tot}}$ . Second, it is generally impossible to obtain an exact analytical relationship to connect  $K$ ,  $E$  and  $R$  with the convergence constraint. In the following section, we propose an algorithm that approximately solves Problem **P1**, which we later show with extensive experiments that the proposed solution can achieve a near-optimal performance of Problem **P1**.

#### IV. COST-EFFECTIVE OPTIMIZATION ALGORITHM

This section shows how to approximately solve Problem **P1**. We first formulate an alternative problem that includes an approximate analytical relationship between the expected cost  $\mathbb{E}[C_{\text{tot}}]$ , the convergence constraint, and the control variables  $E$ ,  $K$  and  $R$ . Then, we show that this new optimization problem can be efficiently solved after estimating unknown parameters associated with the convergence bound, and we propose a sampling-based algorithm to learn these unknown parameters.

##### A. Approximate Solution to Problem **P1**

1) **Analytical Expression of  $\mathbb{E}[e_{\text{tot}}]$** : We first analytically establish the expected energy cost  $\mathbb{E}[e_{\text{tot}}]$  with  $K$  and  $E$ .

**Lemma 1.** *The expectation of  $e_{\text{tot}}$  in (6) can be expressed as*

$$\mathbb{E}[e_{\text{tot}}(K, E, R)] = K(e_p E + e_m)R, \quad (9)$$

where  $e_p := \frac{\sum_{k=1}^N e_{k,p}}{N}$  and  $e_m := \frac{\sum_{k=1}^N \sum_{r=1}^R e_{k,m}^r}{NR}$  denote the average per-device energy consumption for one local iteration and one round of communication, respectively.

*Proof.* Given that all devices are sampled uniformly at random in each round and each round  $K$  out of  $N$  clients are sampled, thus for  $R$  rounds, each device will be sampled in  $\frac{KR}{N}$  rounds in expectation. Based on the result in (5) that each device  $k$  consumes  $e_{k,p}E + e_{k,m}^r$  energy in each round, summing up  $e_{k,p}E + e_{k,m}^r$  over all  $N$  clients and over  $\frac{KR}{N}$  rounds lead to (9).  $\square$

2) **Analytical Expression of  $\mathbb{E}[T_{\text{tot}}]$** : Next, we give an approximate expression of the expected time cost  $\mathbb{E}[T_{\text{tot}}]$  with  $K$  and  $E$ . In the following, we first show how to approximate the per-round time  $T^r$  in (3), based on which we formulate a combinatorial expression of expected  $T_{\text{tot}}$  in (4). Then, we further approximate the expectation of  $T_{\text{tot}}$  for analytical tractability.

Considering that the communication time is usually the bottleneck in wireless FL settings, it is most likely that the maximum in (3) is equal to  $T_{k-1}^r$  for any  $k \in \{2, \dots, K\}$ , e.g., the red shadow time slot in Fig. 1 rarely happens. In other words, the communication channel will be usually occupied after the fastest client (e.g.,  $k = 1$  in the  $K$  clients reordered as in Theorem 1) finishes computation. Therefore,  $T^r$  in (3) can be approximated by

$$T^r \approx t_{1,p}E + \sum_{k=1}^K t_{k,m}^r. \quad (10)$$

Note that the ordering of  $\{t_{k,p} : \forall k \in \mathcal{K}^r\}$  varies across different rounds due to random sampling, i.e., the client with index  $k = 1$  may be different in different rounds. With a slight abuse of notation, we use  $t_{i,p}$  to denote the  $i$ -th fastest client (in terms of computation) out of all  $N$  clients (i.e., before sampling), such that

$$t_{1,p} \leq t_{2,p} \leq \dots \leq t_{i,p} \leq \dots \leq t_{N,p}. \quad (11)$$

**Lemma 2.** *With the reordered clients as in (11) and the approximate  $T^r$  as in (10), the expectation of  $T_{\text{tot}}$  in (4) can be expressed as<sup>6</sup>*

$$\mathbb{E}[T_{\text{tot}}(K, E, R)] \approx \left( \frac{\sum_{i=1}^{N-i+1} C_{N-i}^{i-1} t_{i,p}}{C_N^K} E + t_m K \right) R, \quad (12)$$

where  $t_m := \frac{\sum_{i=1}^N \sum_{r=1}^R t_{i,m}^r}{NR}$  is the average per-device time cost for one round of communication.

We give the full proof in Appendix B. The basic idea is to show the expectation of  $T^r$  in (10) is  $\mathbb{E}[T^r] \approx \frac{\sum_{i=1}^{N-K+1} C_{N-i}^{K-1} t_{i,p}}{C_N^K} E + t_m K$ , where  $\frac{\sum_{i=1}^{N-K+1} C_{N-i}^{K-1} t_{i,p}}{C_N^K} E$  represents that the probability of client  $i$  being the first scheduling client is  $\frac{C_{N-i}^{K-1}}{C_N^K}$ , and the second term  $t_m K$  is derived similar to  $e_m$  in Lemma 1. In particular, the multiplication of  $K$  in  $t_m K$  characterizes the scheduling property of wireless communications with limited bandwidth.

However,  $\mathbb{E}[T_{\text{tot}}]$  in (12) is still hard to analyze due to the various combinatorial terms with respect to control variable  $K$ . For analytical tractability, similar to how we derive (9), we define an approximation of  $\mathbb{E}[T_{\text{tot}}]$  as

$$\tilde{\mathbb{E}}[T_{\text{tot}}(K, E, R)] := (t_p E + t_m K) R, \quad (13)$$

where  $t_p := \frac{\sum_{i=1}^N t_{i,p}}{N}$  is the average per-device time cost for one local iteration. The approximation  $\tilde{\mathbb{E}}[T_{\text{tot}}]$  in (13) is equivalent to  $\mathbb{E}[T_{\text{tot}}]$  in (12) in the following two cases.

*Case 1:* For clients with homogeneous computation capabilities, e.g.,  $t_p = t_{i,p}, \forall i \in \{1, \dots, N\}$ , along with the recursive property of  $C_m^n + C_m^{n-1} = C_{m+1}^n$ , we have

$$\begin{aligned} \mathbb{E}[T_{\text{tot}}(K, E, R)] &= \left( t_p E \frac{\sum_{i=1}^{N-K+1} C_{N-i}^{K-1}}{C_N^K} + t_m K \right) R \\ &= (t_p E + t_m K) R \\ &= \tilde{\mathbb{E}}[T_{\text{tot}}(K, E, R)]. \end{aligned}$$

*Case 2:* For clients with heterogeneous computation capabilities with  $K = 1$ , we have

$$\begin{aligned} \mathbb{E}[T_{\text{tot}}(K = 1, E, R)] &= \left( \frac{\sum_{i=1}^N t_{i,p} E}{N} + t_m K \right) R \\ &= (t_p E + t_m K) R \\ &= \tilde{\mathbb{E}}[T_{\text{tot}}(K = 1, E, R)]. \end{aligned}$$

In the following cost analysis, we use  $\tilde{\mathbb{E}}[T_{\text{tot}}(K, E, R)]$  in (13) as the approximate expected value of the original total learning time in (4).

3) **Analytical Relationship Between  $\mathbb{E}[C_{\text{tot}}]$  and Convergence**: Based on  $\mathbb{E}[e_{\text{tot}}]$  in (9) and the approximation  $\tilde{\mathbb{E}}[T_{\text{tot}}(K, E, R)]$  in (13), we formulate an approximate objective function of Problem **P1** as

$$\tilde{\mathbb{E}}[C_{\text{tot}}] = (\gamma K(e_p E + e_m) + (1 - \gamma)(t_p E + t_m K)) R. \quad (14)$$

<sup>6</sup>The notation of  $C_N^K$  is also noted as  $\binom{N}{K}$  which represents the combination number of choosing  $K$  out of  $N$  without replacement.

To connect  $\tilde{\mathbb{E}}[C_{\text{tot}}]$  with the  $\epsilon$ -convergence constraint in (8) as well as to characterize the heterogeneous data, we utilize the convergence result [10]<sup>7</sup>:

$$\mathbb{E}[F(\mathbf{w}_R)] - F^* \leq \frac{1}{ER} \left( A_0 + B_0 \left( 1 + \frac{N-K}{K(N-1)} \right) E^2 \right), \quad (15)$$

where  $A_0$  and  $B_0$  are loss function related constants characterizing the statistical heterogeneity of non-i.i.d. data. By letting the upper bound satisfy the convergence constraint,<sup>8</sup> we approximate Problem **P1** as

$$\begin{aligned} \mathbf{P2}: \min_{E,K,R} & (\gamma K (e_p E + e_m) + (1-\gamma) (t_p E + t_m K)) R \\ \text{s.t.} & \frac{1}{ER} \left( A_0 + B_0 \left( 1 + \frac{N-K}{K(N-1)} \right) E^2 \right) \leq \epsilon \\ & K, E, R \in \mathbb{Z}^+, \text{ and } 1 \leq K \leq N. \end{aligned} \quad (16)$$

Combining with (15), we can see that Problem **P2** is more constrained than Problem **P1**, as any feasible solution of **P2** is also feasible for **P1**, but not vice versa.

Problem **P2**, however, is a non-linear constrained *integer* optimization problem, which is still difficult to solve in general. Therefore, we relax  $K$ ,  $E$  and  $R$  as continuous variables for theoretical analysis, which are rounded back to integer variables<sup>9</sup> later. For the relaxed problem, if any feasible solution  $E'$ ,  $K'$ , and  $R'$  satisfies the  $\epsilon$ -constraint in Problem **P2** with inequality, we can always decrease this  $R'$  to some  $R''$  ( $R'' < R'$ ), which satisfies the constraint with equality but reduces the objective function value. Hence, for optimal  $R$ , the  $\epsilon$ -constraint is always satisfied with equality, and we can obtain  $R$  from this equality as

$$R = \frac{1}{\epsilon E} \left( A_0 + B_0 \left( 1 + \frac{N-K}{K(N-1)} \right) E^2 \right). \quad (17)$$

By substituting (17) into problem **P2**, we obtain

$$\begin{aligned} \mathbf{P3}: \min_{E,K} & \left( (1-\gamma) (t_p E + t_m K) + \gamma K (e_p E + e_m) \right) \\ & \cdot \frac{A_0 + B_0 \left( 1 + \frac{N-K}{K(N-1)} \right) E^2}{\epsilon E} \\ \text{s.t.} & E \geq 1, \text{ and } 1 \leq K \leq N, \end{aligned} \quad (18)$$

In the following, we solve Problem **P3** as an approximation of the original problem **P1**. Our empirical results in Section VI demonstrate that the solution obtained from solving **P3** achieves *near-optimal performance* of the original problem **P1**. For ease of analysis, we incorporate  $\epsilon$  in the constants  $A_0$  and  $B_0$ .

### B. Solving the Approximate Optimization Problem **P3**

In this subsection, we first characterize some properties of the optimization problem **P3**. Then, we propose a sampling-based algorithm to learn the problem-related unknown parameters  $A_0$  and  $B_0$ , based on which the solution  $K^*$  and  $E^*$  (of Problem **P3**) can be efficiently computed. The overall algorithm for obtaining  $K^*$  and  $E^*$  is given in Algorithm 2.

<sup>7</sup>We use the convergence result in [10] because both [10] and our work analyze the FedAvg algorithm, and the convergence result in [10] includes both control variables  $E$  and  $K$  for cost minimization. We also note that the convergence result in [10] requires clients to decay the learning rate throughout the training process, which we show later in Section VI.

<sup>8</sup>We note that optimization using upper bound as an approximation has also been adopted in [14] and resource allocation based literature [13], [27], [36].

<sup>9</sup>For two integer variables we have four rounding combinations of  $(\lceil K \rceil, \lceil E \rceil)$ ,  $(\lceil K \rceil, \lfloor E \rfloor)$ ,  $(\lfloor K \rfloor, \lceil E \rceil)$ , and  $(\lfloor K \rfloor, \lfloor E \rfloor)$ .

---

### Algorithm 2: Cost-effective design of $K$ and $E$

---

**Input:**  $N, \gamma, t_p, t_m, e_p, e_m$ , loss  $F_a$  and  $F_b$ ,  $\mathbf{w}_0$ , number of sampled pairs  $M$ , stopping condition  $\epsilon_0$   
**Output:**  $K^*$  and  $E^*$

- 1 **for**  $i = 1, 2, \dots, M$  **do**
- 2     Empirically choose  $(K_i, E_i)$  and run Algorithm 1;
- 3     Record  $R_{i,a}$  and  $R_{i,b}$  when  $F_a$  and  $F_b$  are reached;
- 4 Calculate average  $\frac{A_0}{B_0}$  using (22);
- 5 Choose a feasible  $z_0 \leftarrow (K_0, E_0)$  and set  $j \leftarrow 0$ ;
- 6 **while**  $\|z_j - z_{j-1}\| > \epsilon_0$  **do**
- 7     Substitute  $E_j, \frac{A_0}{B_0}, N, \gamma, t_p, t_m, e_p, e_m$  into (18) and derive  $K'$ ;
- 8      $K_{j+1} \leftarrow \arg \min_{K \in [1, N]} |K - K'|$ ;
- 9     Substitute  $K_{j+1}, \frac{A_0}{B_0}, N, \gamma, t_p, t_m, e_p, e_m$  into (18) and derive  $E'$ ;
- 10     $E_{j+1} \leftarrow \arg \min_{E \geq 1} |E - E'|$ ;
- 11     $z_{j+1} \leftarrow (K_{j+1}, E_{j+1})$  and  $j \leftarrow j + 1$ ;
- 12 Substitute four rounding combinations of  $(\lceil K_j \rceil, \lceil E_j \rceil)$ ,  $(\lceil K_j \rceil, \lfloor E_j \rfloor)$ ,  $(\lfloor K_j \rfloor, \lceil E_j \rceil)$ , and  $(\lfloor K_j \rfloor, \lfloor E_j \rfloor)$  into the objective function of problem **P3**, and set the pair with the minimum value as  $(K^*, E^*)$
- 13 **return**  $(K^*, E^*)$

---

#### 1) Characterizing Problem **P3**:

**Theorem 2.** *Problem **P3** is strictly biconvex [45].*

*Proof.* For any  $E \geq 1$ , we have

$$\frac{\partial^2 \tilde{\mathbb{E}}[C_{\text{tot}}]}{\partial^2 K} = \frac{2(1-\gamma)B_0 N t_p E^2}{(N-1)K^3} > 0.$$

Similarly, for any  $1 \leq K \leq N$ , we have

$$\begin{aligned} \frac{\partial^2 \tilde{\mathbb{E}}[C_{\text{tot}}]}{\partial^2 E} &= 2 \left( (1-\gamma) t_p + \gamma K e_p \right) B_0 \left( 1 + \frac{N-K}{K(N-1)} \right) \\ &+ \frac{2A_0 \left( (1-\gamma) K t_m + \gamma K e_m \right)}{E^3} > 0 \end{aligned} \quad (19)$$

Since the domain of  $K$  and  $E$  is convex, we conclude that Problem **P3** is strictly biconvex.  $\square$

The biconvex property allows many efficient algorithms, such as *Alternate Convex Search* (ACS) approach, to achieve a guaranteed local optima [45]. E.g., we could iteratively solve  $K$  and  $E$  in the objective function (18) until we achieve the converged  $K^*$  and  $E^*$ . This optimization process corresponds to Lines 5–13 of Algorithm 2, where Lines 8 and 10 ensure that the solution is taken within the feasibility region, and Line 12 rounds the continuous values of  $K$  and  $E$  to integer values.

2) *Estimation of Parameters  $\frac{A_0}{B_0}$* : Solving the objective function (18) is still nontrivial because it includes unknown parameters  $A_0$  and  $B_0$ , which can only be determined during the learning process.<sup>10</sup> In fact, the optimal  $K$  and  $E$  in (18) only depend on the value of  $\frac{A_0}{B_0}$  as we could divide  $B_0$  and incorporate it in  $\epsilon$ . In the following, we propose a sampling-based algorithm to estimate  $\frac{A_0}{B_0}$ , and show that the overhead for estimation is marginal.

The basic idea is to sample different combinations of  $(K, E)$  and use the upper bound in (15) to approximate  $F(\mathbf{w}_R) - F^*$ . Specifically, we empirically sample<sup>11</sup> a pair  $(K_i, E_i)$  and run

<sup>10</sup>We assume that  $t_p, t_m, t_m$  and  $e_m$  can be measured offline.

<sup>11</sup>Our sampling criteria is to cover diverse combinations of  $(K, E)$ .

Algorithm 1 with an initial model  $\mathbf{w}_0 = \mathbf{0}$  until it reaches two pre-defined global losses  $F_a := F(\mathbf{w}_{R_{i,a}})$  and  $F_b := F(\mathbf{w}_{R_{i,b}})$  ( $F_b < F_a$ ), where  $R_{i,a}$  and  $R_{i,b}$  are the executed round numbers for reaching losses  $F_a$  and  $F_b$ . The pre-defined losses  $F_a$  and  $F_b$  can be set to a relatively high value, to keep a small estimation overhead, but they cannot be too high either as it would cause low estimation accuracy. Then, we have

$$\begin{cases} R_{i,a} \approx d + \frac{A_0 + B_0 \left(1 + \frac{N-K_i}{K_i(N-1)}\right) E_i^2}{E_i (F_a - F^*)}, \\ R_{i,b} \approx d + \frac{A_0 + B_0 \left(1 + \frac{N-K_i}{K_i(N-1)}\right) E_i^2}{E_i (F_b - F^*)}. \end{cases} \quad (20)$$

from (15), where  $d$  captures a constant error of using the upper bound to approximate  $F(\mathbf{w}_R) - F^*$ . Based on (20), we have

$$R_{i,b} - R_{i,a} \approx \frac{\Delta}{E_i} \left( A_0 + B_0 \left(1 + \frac{N-K_i}{K_i(N-1)}\right) E_i^2 \right), \quad (21)$$

where  $\Delta := \frac{1}{F_b - F^*} - \frac{1}{F_a - F^*}$ . Similarly, sampling another pair of  $(K_j, E_j)$  and performing the above process gives us another executed round numbers  $R_{j,a}$  and  $R_{j,b}$ . Thus, we have

$$\frac{E_i (R_{i,b} - R_{i,a})}{E_j (R_{j,b} - R_{j,a})} \approx \frac{A_0 + B_0 \left(1 + \frac{N-K_i}{K_i(N-1)}\right) E_i^2}{A_0 + B_0 \left(1 + \frac{N-K_j}{K_j(N-1)}\right) E_j^2}. \quad (22)$$

We can obtain  $\frac{A_0}{B_0}$  from (22) (note that the variables except for  $\frac{A_0}{B_0}$  are known). In practice, we may sample several different pairs of  $(K_i, E_i)$  to obtain an averaged estimation of  $\frac{A_0}{B_0}$ . This estimation process is given in Lines 1–4 of Algorithm 2.

**Estimation overhead:** The main overhead used for estimation  $\frac{A_0}{B_0}$  comes from the additional iterations with different sampling pairs  $(K_i, E_i)$ . For each pair,  $K_i$  clients conduct  $R_{i,b}$  rounds of  $E_i$  step local iterations for reaching the lower pre-defined loss  $F_b$ . Hence, for  $M$  sampling pairs, the number of iteration  $I_{est}$  used for estimation is

$$I_{est} = \sum_{i=1}^M K_i E_i R_{i,b}. \quad (23)$$

For training with obtained  $(K^*, E^*)$ , then according to (15), the total iteration number  $I_{tot}$  that used for reaching  $\epsilon = F_R - F^*$  precision is

$$I_{tot} = K^* E^* R \approx \frac{K^* \left[ A_0 + B_0 \left(1 + \frac{N-K^*}{K^*(N-1)}\right) (E^*)^2 \right]}{\epsilon}. \quad (24)$$

Therefore, the estimation overhead ratio can be expressed as

$$\frac{I_{est}}{I_{tot}} \approx \epsilon \cdot \frac{\sum_{i=1}^M K_i E_i R_{i,b}}{K^* \left[ A_0 + B_0 \left(1 + \frac{N-K^*}{K^*(N-1)}\right) (E^*)^2 \right]}, \quad (25)$$

where the right hand side of (25) except for  $\epsilon$  is bounded by some constant value, and thus the overhead ratio will be marginal for a high error precision with  $\epsilon$  being small.

## V. DESIGN PRINCIPLES AND SOLUTION PROPERTIES FOR COST MINIMIZATION

We theoretically analyze the solution properties for different optimization metrics and heterogeneous system parameters. The analysis not only provides insightful design principles but also gives alternative ways of solving Problem **P3** more efficiently. Our empirical results in Section VI show that these properties derived for Problem **P3** are still valid for the original problem **P1**. For the ease of presentation, we consider continuous  $K$  and  $E$  (i.e., before rounding) in this section.

### A. Solution Property of $K$ for Minimizing $\tilde{\mathbb{E}}[C_{tot}]$

We first show how the normalized price factor  $\gamma$  affects the optimal solution of  $K$ . This provides useful design principles for choosing the number of participants for different optimization metrics, e.g., learning time or energy minimization.

**Theorem 3.** *For any fixed value of  $E$ ,  $K^*$  decreases in  $\gamma$ . In particular, when  $\gamma = 1$ ,  $\tilde{\mathbb{E}}[C_{tot}]$  is a strictly increasing function in  $K$ , thus  $K^* = 1$ .*

The proof is given in Appendix C. Theorem 3 shows that sampling fewer devices can reduce the total energy consumption for reaching the target loss (which would be the main objective as  $\gamma$  becomes large). While this may seem contradictory at the first glance, since a smaller  $K$  would result in more rounds to achieve the desired precision  $\epsilon$ . The key intuition is that the total energy is the sum energy consumption of all selected clients. Although more rounds may cost longer learning time, there are also less number of clients participating in each round, so the total energy consumption can be smaller. Particularly, for pure energy minimization task ( $\gamma = 1$ ) with  $K^* = 1$ , our proposed sequential ordering scheduling in Theorem 1 reduces to uniformly at random sample one client for transmission in each round, which is a bit different compared to the Round-Robin scheme, because the sequence of our selected clients over several rounds is random not always following the same order.

Based on Theorem 3, we derive a trade-off design principle for  $K$ , generally, with a relatively larger<sup>12</sup>  $K$  favoring learning time reduction (small  $\gamma$ ) and a smaller  $K$  favoring energy saving (large  $\gamma$ ). For a given  $\gamma$ , the optimal  $K^*$  achieves the best balance between learning time minimization and energy consumption minimization.

Next, we show how heterogeneous system parameters in terms of computation and communication affect the optimal solution of  $K$ . This shows which directions  $K$  and  $E$  should change to, when the system environment changes.

**Theorem 4.** *For any fixed value of  $E$ , when  $0 < \gamma < 1$ ,  $K^*$  increases in  $t_p$  and decreases in  $t_m$ ,  $e_p$  and  $e_m$ . When  $\gamma = 0$ ,  $K^*$  increases with  $\frac{t_p}{t_m}$ ; whereas when  $\gamma = 1$ ,  $K^*$  is independent of  $e_m$  and  $e_p$ .*

We give the proof in Appendix D. Intuitively, for general  $0 \leq \gamma < 1$ , Theorem 4 says that when  $t_m$  increases (e.g.,

<sup>12</sup>We note that the main difference for reducing time cost between this work and wired FL in [1] is that the optimal  $K^*$  (for  $\gamma = 0$ ) in [1] is always  $N$ , where it is usually some value between  $[1, N]$  in this paper.



more clients suffering poor channel conditions or less system bandwidth is available), or  $e_m$  and  $e_p$  increases (higher average energy costs in communication or computation), the optimal strategy to reduce the total cost is to sample fewer clients. Interestingly, when the average computation time  $t_p$  increases, we should sample more clients. This is because, unlike the per-round communication time accumulated with more clients being sampled, the computation is performed in parallel among the sampled clients, which only slightly increases the per-round time. Sampling more clients can possibly reduce the required total number of rounds, thus bringing down the total learning time. When we only focus on energy minimization ( $\gamma = 1$ ), the optimal  $K$  is independent of  $e_m$  and  $e_p$ , because Theorem 3 shows that  $K^* = 1$  in this case.

### B. Solution Property of $E$ for Minimizing $\tilde{\mathbb{E}}[C_{\text{tot}}]$

We first identify how the normalized price factor  $\gamma$  affects the choice of  $E$  for different optimization goals, e.g., learning time or energy minimization.

**Theorem 5.** For any  $0 \leq \gamma \leq 1$  and any fixed value of  $K$ , as  $E$  increases,  $\tilde{\mathbb{E}}[C_{\text{tot}}]$  first decreases and then increases.

The proof is given in Appendix E. Theorem 5 shows that, unlike the strategy for minimizing energy consumption where  $K^*$  lies at the boundary, the optimal  $E$  should not be set too small nor too large no matter for saving energy consumption or learning time.

Then, the following theorem characterizes how heterogeneous system parameters in computation and communication affect the design principle of optimal  $E$ .

**Theorem 6.** For any fixed value of  $E$ , when  $0 < \gamma < 1$ ,  $E^*$  increases as  $t_p$  or  $e_p$  decreases.  $E^*$  increases in  $\frac{t_m}{t_p}$  when  $\gamma = 0$ , and  $E^*$  increases in  $\frac{e_m}{e_p}$  when  $\gamma = 1$ .

We give the proof in Appendix F. Theorem 6 says that for any given  $K$ , when  $t_p$  or  $e_p$  decreases, the optimal strategy for learning time minimization ( $\gamma = 0$ ) or energy consumption minimization ( $\gamma = 1$ ) is to perform more steps of iterations (i.e., increase  $E$ ) before aggregation. This is because when computation is cheaper or when communication is more expensive, it is beneficial to perform more computation in each round, as intuition suggests. This theorem provides theoretical evidence for the empirical observations in [7], [15]–[17].

## VI. EXPERIMENTAL EVALUATION

In this section, we evaluate the performance of our proposed scheduling scheme, cost-effective FL algorithm and derived solution properties. We start by presenting the evaluation setup, and then show the experimental results.

### A. Experimental Setup

1) *Platforms*: We conducted experiments both on a networked hardware prototype system and in a simulated environment. Our prototype system, as illustrated in Fig. 2, consists of 30 edge devices with 20 Raspberry Pis (version 4) and 10 Jetson Nanos as well as a laptop computer serving as the

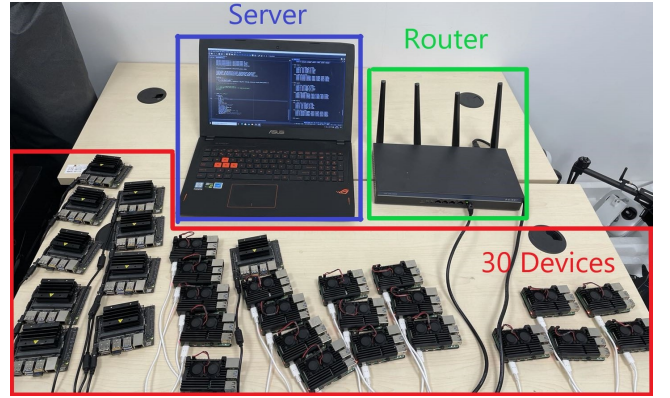


Fig. 2. Hardware prototype with the laptop being central server, 20 Raspberry Pi and 10 Jetson Nano being devices. During the FL experiments, the wireless router is placed 2 meters away from all the devices.

central server. All devices are interconnected via an enterprise Wi-Fi router, and we developed a TCP-based socket interface for the peer-to-peer connection.<sup>13</sup> In the simulation system, we simulated a cellular network of an urban microcell consisting of a central BS serving as the server and  $N = 100$  clients. The BS and server were co-located at the center of the cell with a radius of 2 km, and the clients were uniformly distributed in the cell.

2) *Datasets and Models*: We evaluate our results both on a real dataset and a synthetic dataset. For the real dataset, following a same setup of [46], we adopted the widely used MNIST dataset and EMNIST dataset, which contains gray-scale images of handwritten digits and characters. For the synthetic dataset, we follow a similar setup to that in [21], which generates 60-dimensional random vectors as input data. The synthetic data is denoted by *Synthetic*  $(\alpha, \beta)$  with  $\alpha$  and  $\beta$  representing the statistical heterogeneity (i.e., how non-i.i.d. the data are). We adopt the *convex* multinomial logistic regression model for both datasets with model size around 0.03 MB [10].

3) *Implementation*: Based on the above, we consider the following three experimental setups with heterogeneous data distribution.

*Prototype Setup*: We conduct the first experiment on the prototype system using MNIST dataset, where we divide 9,000 data samples among the  $N = 30$  edge devices (20 Raspberry Pis and 10 Jetson Nanos) in a non-i.i.d. fashion, with each device containing a balanced number of 300 samples of only 2 digit labels.

*Simulation Setup 1*: We conduct the second experiment in the simulated system using EMNIST dataset, where we divide 48,000 image samples among  $N = 100$  clients in a non-i.i.d. fashion, with each client containing a balanced number of 480 samples of only 2 classes.

*Simulation Setup 2*: We conduct the third experiment in the simulated system using *Synthetic*  $(1, 1)$  dataset for statistical heterogeneity. We generate 24,517 data samples and distribute

<sup>13</sup>To characterize LTE-based wireless networks as in Fig. 1, we manually change the original communication protocol in our TS-based WiFi system, so that all devices start their local training at the same time and without calculating the downlink time.

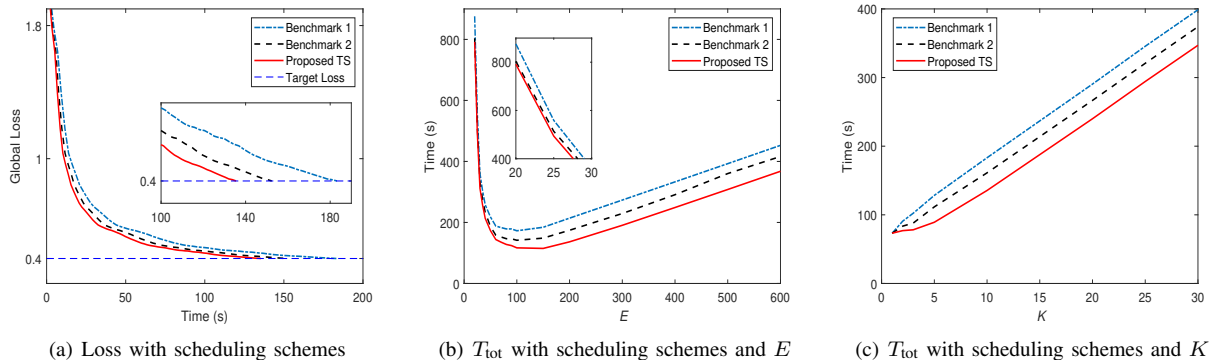


Fig. 3. Total learning time performance of **Prototype Setup** for different scheduling strategies with logistic regression and MNIST dataset. (a): For a given pair ( $K = 10, E = 70$ ), our proposed scheduling strategy achieves the target loss 0.4 faster than the two benchmark schemes. (b): For fixed  $K = 10$ , our proposed scheme achieve the target loss using shorter time for different  $E$ . (c): For fixed  $E = 70$ , our proposed scheme achieve the target loss using shorter time for different  $K$ .

them among  $N = 100$  mobile devices in an unbalanced power law distribution, where the number of samples in each device has a mean of 245 and standard deviation of 362.

4) *Training Parameters*: For all experiments, we initialize our model with  $\mathbf{w}_0 = \mathbf{0}$  and SGD batch size  $b = 64$ . In each round, we uniformly sample  $K$  devices at random, which run  $E$  steps of SGD in parallel. For all experiments, we use an initial learning rate  $\eta_0 = 0.1$  with decay rate  $\frac{\eta_0}{1+r}$ , where  $r$  is communication round index. We evaluate the aggregated model in each round on the global loss function. Each result is averaged over 50 experiments.

5) *Heterogeneous System Parameters*: The prototype system allows us to capture real system heterogeneity in terms of communication and computation time, which we measured the average  $t_p = 4.9 \times 10^{-3}$  s with standard deviation  $1.43 \times 10^{-3}$  s and  $t_m = 0.16$  s with standard deviation 0.03 s. We do not consider the energy cost in the prototype system because it is difficult to measure. For the simulated mobile edge system, we assume the system bandwidth is 1.8 MHz and adopt the standard LTE communications model based on a well-known urban channel model with the mean per-client throughput 1.4 Mbit/s (thus  $t_m \approx 0.2$  s) as in [29]. We generate the computation time and energy consumption for each client using a truncated normal distribution with mean value of  $t_p = 0.5$  s (emulating slow devices),  $e_p = 0.01$  J, and  $e_m = 0.02$  J. According to the definition of  $\gamma$ , we unify the time and energy costs such that one second is equivalent to  $1 - \gamma$  dollars (\$) and one Joule is equivalent to  $\gamma$  dollars (\$).

## B. Performance Results

In this subsection, we first evaluate the performance of our proposed TS scheduling strategy with two existing benchmarks. Then, we compare the performance of the proposed solution ( $K^*, E^*$ ) obtained from Algorithm 2 for solving Problem **P3**, with that of the empirical optimal solution ( $K_{\text{OPT}}, E_{\text{OPT}}$ ) achieved by an exhaustive search on the optimal solution of the original problem **P1**. Finally, we validate our derived design principles and solution properties.

1) *Scheduling Performance*: Fig. 3 compares the total learning time **performance of our proposed TS scheduling with the following two benchmarks** in Prototype Setup:

- Benchmark 1: existing TS scheduling strategy in [13], where communication does not begin until all sampled clients complete their local computations.
- Benchmark 2: existing FS scheduling strategy in [27], [30], [36], where the algorithm allocates the bandwidth at the start of each round for the sampled clients, then the bandwidth allocation remains unchanged throughout the round and every selected client starts its communication using its allocated bandwidth whenever its computation has finished.

The main observations are as follows.

- Fig. 3 demonstrates that *our proposed scheduling strategy in Theorem 1 achieves the target loss faster than the two benchmarks*, since our method can better utilize system resources and adapt to both computation and communication heterogeneity.
- *The performance gaps between our scheme and the two benchmarks increase in  $E$  at first and then remain stable in Fig. 3(b)*. The reason for this observation is that, as  $E$  increases, the computation times between different sampled clients are more different, allowing our scheme to better utilize the full bandwidth and thus save per-round time. When  $E$  is large enough, the per-round time is only dominated by computation time, hence the impact of different scheduling is insignificant as scheduling mainly affects the communication time.
- We also observe that *the performance gaps between our scheme and the two benchmarks increase in  $K$  at first and then remain stable in Fig. 3(c)*. The explanation for this observation is that as  $K$  increases, the difference between the maximum and minimum computation time among the selected  $K$  clients can be larger, allowing our scheme to better utilize the computational heterogeneity, e.g., communication could begin at an early stage instead of waiting for the rest clients. When  $K$  is large enough, the per-round time is mainly dominated by communication

TABLE III  
NUMBER OF ROUNDS FOR REACHING ESTIMATION LOSS  $F_a$  AND  $F_b$  FOR ESTIMATION OF  $\frac{A_0}{B_0}$  FOR THREE SETUPS

Prototype Setup MNIST	Estimation loss $F_a = 0.65$ $F_b = 0.55$	Samples of $(K, E)$					Estimated $\frac{A_0}{B_0} = 36,500$	
		(1, 30)	(5, 80)	(10, 40)	(15, 100)	(20, 50)		
Simulation Setup 1 EMNIST	Estimation loss $F_a = 1.2$ $F_b = 1.0$	Rounds to achieve $F_a$	50	17	17	13	14	Estimated $\frac{A_0}{B_0} = 960$
		Rounds to achieve $F_b$	75	32	30	21	25	
Simulation Setup 2 Synthetic (1,1)	Estimation loss $F_a = 1.7$ $F_b = 1.5$	Rounds to achieve $F_a$	41	28	22	19	18	Estimated $\frac{A_0}{B_0} = 1850$
		Rounds to achieve $F_b$	78	52	39	34	31	

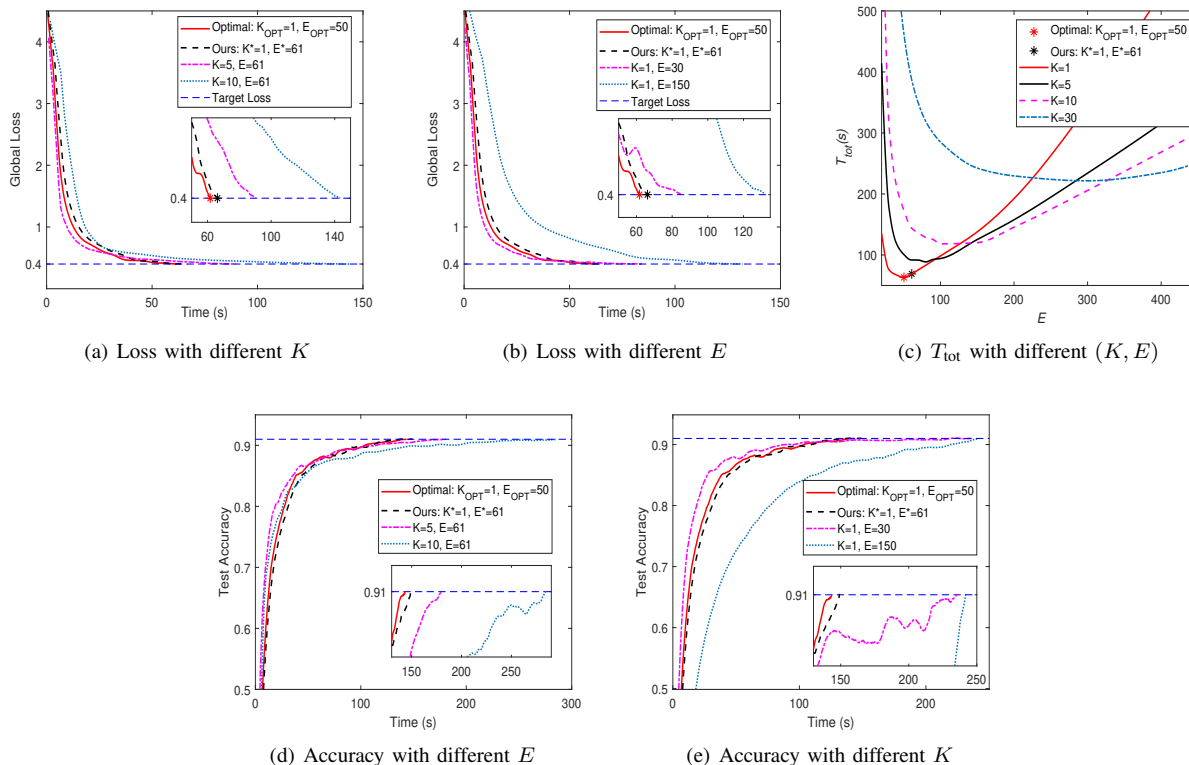


Fig. 4. Training performance of  $T_{\text{tot}}$  for **Prototype Setup** with logistic regression and MNIST dataset for  $\gamma=0$ . (a)-(c): Our solution achieves the target loss using 66.2 s compared to the empirical optimum 61.7 s, but faster than those with  $E$  being too small or too large and those with  $K$  being large. (d)-(e): Our solution achieves target test accuracy 91% slightly longer than the optimal solution, but faster than the non-optimal values of  $(K, E)$  in (a) and (b).

time, and the gain from computational heterogeneity tends to be stable between different scheduling schemes.

2) *Optimality Performance*: We first present the estimation process and results of  $\frac{A_0}{B_0}$  for the three experiment setups in Table III. Figs. 4–6 compare the **performance of our proposed solution of  $(K^*, E^*)$  with empirical optimal solution  $(K_{\text{OPT}}, E_{\text{OPT}})$**  and other  $(K, E)$  pairs<sup>14</sup> for Prototype

and Simulation Setups, respectively.<sup>15</sup> The key observations are as follows.

- Fig. 4 shows the learning time cost  $T_{\text{tot}}$  for reaching the target loss under different  $(K, E)$  for Prototype Setup.<sup>16</sup> In particular, *our solution achieves the target loss using 66.2 s compared to the empirical optimum 61.7 s*, whereas other  $(K, E)$  pairs without optimization may

<sup>15</sup>We note that  $(K^*, E^*)$  are obtained by estimating the average value of  $\frac{A_0}{B_0}$ , whose estimation process is summarized in Table III. Specifically, we empirically set two relatively high target losses  $F_a$  and  $F_b$  with a few sampling pairs of  $(K, E)$ . Note that due to different learning tasks and statistical heterogeneity, the sampling range of  $E$  in Prototype Setup is larger than that in Simulation Setup. Then, we record the corresponding number of rounds for reaching  $F_a$  and  $F_b$ , based on which we calculate the averaged estimation value of  $\frac{A_0}{B_0}$  using (22).

<sup>14</sup>The benchmark  $E$  and  $K$  are chosen to be either larger or smaller than the empirical optimal ones for comparison.

<sup>16</sup>For hardware prototype, we only show the convergence performance with  $T_{\text{tot}}$  for  $\gamma = 0$ .

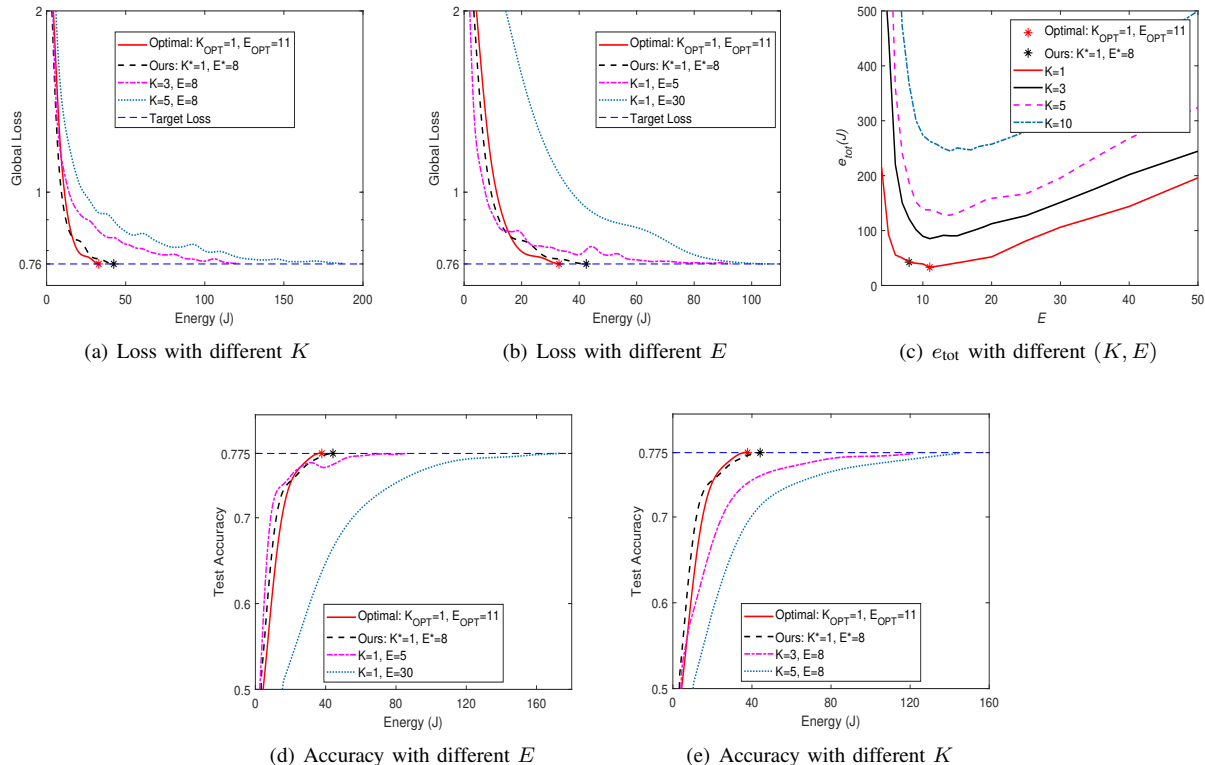


Fig. 5. Training performance of  $e_{\text{tot}}$  for **Simulation Setup 1** with logistic regression and EMNIST dataset for  $\gamma = 1$ . (a)-(c): Our solution achieves the target loss using 42.4 J, which is slightly larger than the empirical optimum 33.7 J, but saves several folds of energy compared to those  $(E, K)$  pairs without optimization. (d-e): Our solution achieves the target test accuracy 77.5% using slightly more energy than the optimal solution, but saves several folds of energy than the non-optimal values of  $(K, E)$  in (a) and (b).

consume a learning time that is several folds more, as shown in Fig. 4(c).<sup>17</sup>

- Fig. 5 depicts the energy cost  $e_{\text{tot}}$  for reaching the target loss under different  $(K, E)$  for Simulation Setup 1. *Our solution achieves the target loss and accuracy with the similar energy cost compared to the empirical optimal solution, and saves several folds of energy compared to those  $(K, E)$  pairs without optimization.*
- Figs. 6 shows the total cost  $C_{\text{tot}}$  for reaching the target loss for different  $\gamma$  under different  $(K, E)$  for Simulation Setup 2. Comparing to other  $(K, E)$  pairs without optimization in Fig. 6(c)-(f), our proposed solutions incur a similar total cost as the corresponding empirical optimal ones through the entire range of  $\gamma$ .

3) **Property Validation:** We highlight that **our derived theoretical properties of  $K$  and  $E$  can be validated empirically** in both prototype and simulation experiments. Particularly, we manually decrease  $t_p$  and  $e_p$  in Simulation Setup 2, and shows how system parameters affect the design principles in Fig. 7. We summarize the key results as follows.

- We observe from Figs. 6(d)-6(e) that the optimal  $K$  decreases from 10 to 1 as  $\gamma$  increases from 0 to 1.

<sup>17</sup>The intersections in Fig. 4(c) and Fig. 5(d) show that, for a given  $E$ , different numbers of  $K$  may result in the same total learning time. This is because the trade-off between the total number of rounds for reaching the target loss and the per-round time, as a large  $K$  reduces the number of rounds but yields a longer per-round time, whereas a small  $K$  reduces the per-round time but requires more rounds.

Particularly, we see from Figs. 5(c) and 6(e) that, when  $\gamma = 1$ , the energy cost strictly increases in  $K$ , with  $K_{\text{OPT}} = 1$ . These observations confirm our claim in Theorem 3.

- Figs. 4(c), 5(c), 6(c)–6(e) demonstrate that for any fixed value of  $K$ , the corresponding total cost first decreases and then increases as  $E$  increases, which confirms our Theorem 5.
- Comparing Fig. 7(a) with Fig. 6(d), we observe that for a fixed value of  $E$ , the optimal  $K$  decreases as  $t_p$  decreases. For example, for  $E = 26$ , the optimal  $K$  decreases from 10 to 2 as  $t_p$  decreases, which confirms Theorem 4.
- Comparing Fig. 7(b) with Fig. 6(e), for fixed value of  $K$ , the optimal  $E$  increases as  $e_p$  decreases, e.g., for  $K = 1$ , the optimal  $E$  increases from 14 to 20, which confirms Theorem 6.

## VII. CONCLUSION

In this work, we have studied the cost-effective design for federated learning in mobile edge networks. We proposed a new time-sharing scheduling scheme which captures system heterogeneity in terms of computation and wireless communication, and analyzed how to optimally choose the number of participating clients ( $K$ ) and the number of local iterations ( $E$ ), which are two essential control variables in FL, to minimize the total cost while ensuring convergence. We proposed a sampling-based control algorithm which efficiently solves

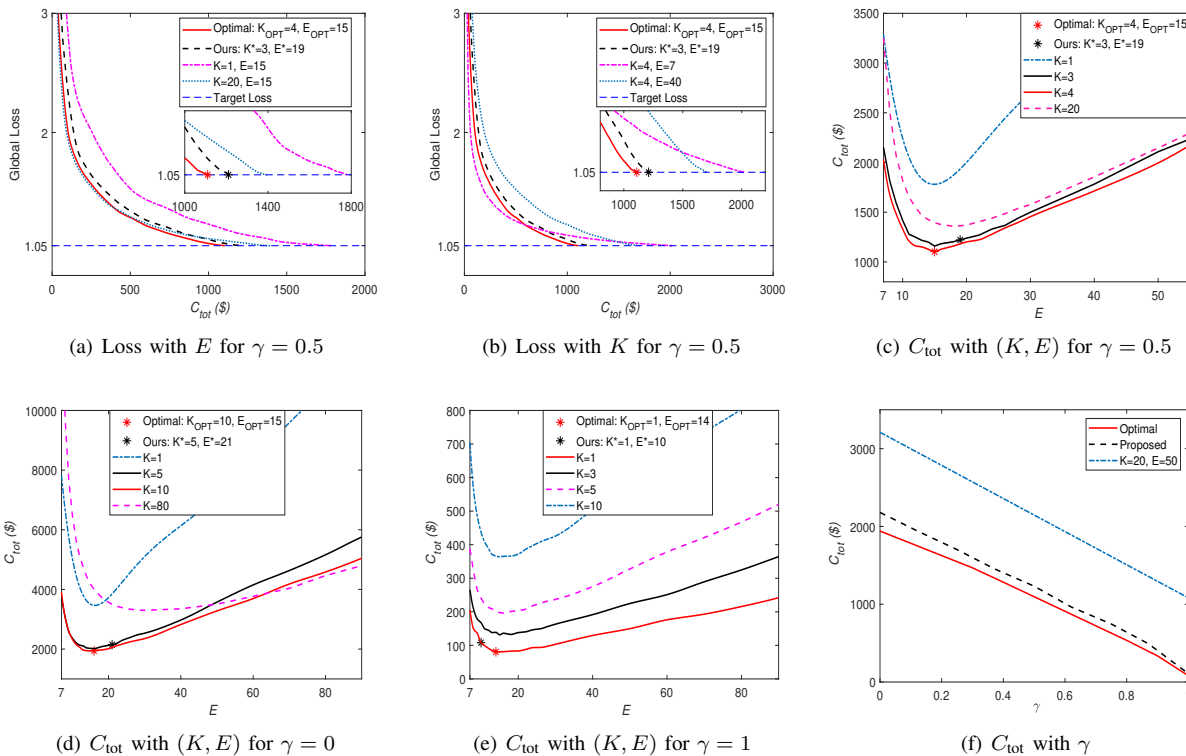


Fig. 6. Performance of  $C_{\text{tot}}$  for reaching the target loss 1.05 for different  $\gamma$  for **Simulation Setup 2** with logistic regression and Synthetic (1,1). (a)-(b): When  $\gamma = 0.5$  our solution reaches the target loss 1.05 using \$1221 compared to the empirical optimal \$1104. (c)-(f): When  $\gamma$  increases from 0 to 1, our proposed solutions reach the target loss using the similar total cost as the corresponding empirical optimal ones.

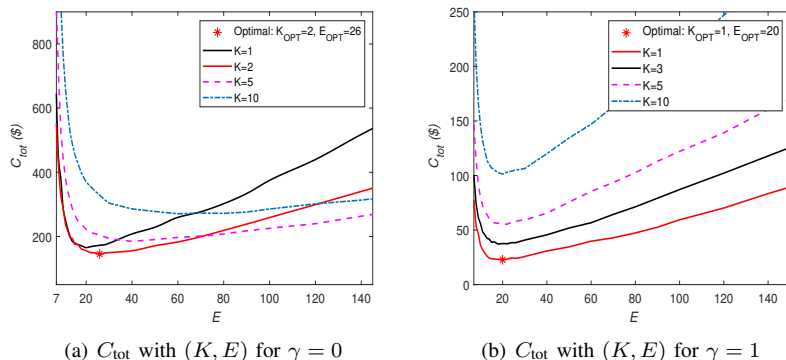


Fig. 7. Performance of  $C_{\text{tot}}$  for reaching the target loss 1.05 for (a)  $\gamma = 0$  and (b)  $\gamma = 1$  for **revised Simulation Setup 2**, where we manually decrease  $t_p$  from 0.5 s to 0.1 s and  $e_p$  from 0.01 J to 0.002 J.

the optimization problem with marginal overhead. We also derived insightful solution properties which helps identify the design principles for different optimization goals, e.g., reducing learning time or saving energy. Extensive experimentation results validated our theoretical analysis and demonstrated the effectiveness and efficiency of our control algorithm. Our optimization design is orthogonal to most works on resource allocation for FL systems, e.g, transmission power or CPU frequency, and can be used together with those techniques to further reduce the cost.

## APPENDIX A PROOF OF THEOREM 1

We prove by contradiction. For any reordered clients sequence  $i-2, i-1$  and  $i$  with  $t_{i-2,p} > t_{i-1,p} > t_{i,p}$ , then the time after scheduling the three clients is:

$$\begin{aligned} T_i &= \max\{t_{i,p}, T_{i-1}\} + t_{i,m} \\ &= \max\{t_{i,p}, \max\{t_{i-1,p}, T_{i-2}\} + t_{i-1,m}\} + t_{i,m}. \end{aligned} \quad (26)$$

Now, suppose we switch the scheduling order of  $i-1$  and  $i$ , then the time after scheduling the three clients is:

$$T'_{i-1} = \max\{t_{i-1,p}, \max\{t_{i,p}, T_{i-2}\} + t_{i,m}\} + t_{i-1,m}. \quad (27)$$

Case 1: if  $t_{i,p} > t_{i-1,p} > T_{i-2}$ , then  $T_i$  in (26) reduces to

$$T_i = \max \{t_{i,p}, t_{i-1,p} + t_{i-1,m}\} + t_{i,m}, \quad (28)$$

and  $T'_{i-1}$  in (27) reduces to

$$\begin{aligned} T'_{i-1} &= \max \{t_{i-1,p}, t_{i,p} + t_{i,m}\} + t_{i-1,m} \\ &= t_{i,p} + t_{i,m} + t_{i-1,m} \\ &> \max \{t_{i,p}, t_{i-1,p} + t_{i-1,m}\} + t_{i,m} = T_i. \end{aligned} \quad (29)$$

Case 2: if  $T_{i-2} > t_{i,p} > t_{i-1,p}$ , then  $T_i$  in (26) reduces to

$$\begin{aligned} T_i &= \max \{t_{i,p}, T_{i-2} + t_{i-1,m}\} + t_{i,m} \\ &= T_{i-2} + t_{i-1,m} + t_{i,m}, \end{aligned} \quad (30)$$

and  $T'_{i-1}$  in (27) reduces to

$$\begin{aligned} T'_{i-1} &= \max \{t_{i-1,p}, T_{i-2} + t_{i,m}\} + t_{i-1,m} \\ &= T_{i-2} + t_{i-1,m} + t_{i,m} = T_i. \end{aligned} \quad (31)$$

Case 3: if  $t_{i,p} > T_{i-2} > t_{i-1,p}$ , then  $T_i$  in (26) reduces to

$$T_i = \max \{t_{i,p}, T_{i-2} + t_{i-1,m}\} + t_{i,m}, \quad (32)$$

and  $T'_{i-1}$  in (27) reduces to

$$\begin{aligned} T'_{i-1} &= \max \{t_{i-1,p}, t_{i,p} + t_{i,m}\} + t_{i-1,m} \\ &= t_{i,p} + t_{i,m} + t_{i-1,m} \\ &> \max \{t_{i,p}, T_{i-2} + t_{i-1,m}\} + t_{i,m} = T_i. \end{aligned} \quad (33)$$

Therefore, we conclude that if any clients are not scheduled based on increasing order of  $t_{k,p}$ , scheduling the same sampled clients would result in a longer time.

#### APPENDIX B PROOF OF LEMMA 2

Since the  $K$  clients are sampled uniformly at random in each round *without replacement*, the ‘‘first’’ scheduling client is  $\min_{k \in \mathcal{K}^r} \{t_{k,p}\}$ . Thus, in the reordered sequence (11), those who could be served as the first are the  $\{1, 2, \dots, N-K+1\}$ th clients.

The probability of client  $i \in \{1, 2, \dots, N-K+1\}$  being the ‘‘first’’ client is  $\frac{C_{N-i}^{K-1}}{C_N^K}$ , where  $C_N^K$  is the number of all possible  $K$  clients combinations,  $C_{N-k}^{K-1}$  is the number of  $K$  clients combinations with client  $i$  being the ‘‘first’’ (fast) client. In other words, the rest  $K-1$  clients must be taken from the behind the  $N-K$  clients who placed behind client  $k$ . Therefore, the expected time of the ‘‘first’’ client is

$$\mathbb{E}[\min_{k \in \mathcal{K}^r} \{t_{k,p}E\}] = \frac{\sum_{i=1}^{N-K+1} C_{N-i}^{K-1} t_{i,p} E}{C_N^K}. \quad (34)$$

Then, similar to the proof in *Lemma 1*, for uniform at random sampling, the probability of each client being sampled in each round is  $\frac{K}{N}$ . Thus, we have

$$\begin{aligned} \mathbb{E}[\sum_{k=1}^K t_{k,m}^r] &= \frac{K}{N} \mathbb{E}[\sum_{i=1}^N t_{i,m}^r] \\ &= K \frac{\sum_{i=1}^N \mathbb{E}[t_{i,m}^r]}{N} = K \frac{\sum_{i=1}^N \bar{t}_{i,m}}{N} = t_m K. \end{aligned} \quad (35)$$

Given that the computation time and communication time are independent, the approximate per-round time in (10) can be expressed as

$$\begin{aligned} \mathbb{E}[T^r] &= \mathbb{E}[\min_{k \in \mathcal{K}^r} \{t_{k,p}E\}] + \mathbb{E}[\sum_{k=1}^K t_{k,m}^r] \\ &= \frac{\sum_{i=1}^{N-K+1} C_{N-i}^{K-1} t_{i,p} E}{C_N^K} + t_m K. \end{aligned} \quad (36)$$

Therefore, (12) can be obtained for  $R$  round communications, which concludes this proof.

#### APPENDIX C PROOF OF THEOREM 3

Taking the first order derivative of  $\tilde{\mathbb{E}}[C_{\text{tot}}]$  over  $K$  for any given  $E$ , we have

$$\begin{aligned} \frac{\partial \tilde{\mathbb{E}}[C_{\text{tot}}]}{\partial K} &= [(1-\gamma)t_m + \gamma(e_p E + e_m)] \left( \frac{A_0}{E} + \frac{B_0(N-2)E}{N-1} \right) \\ &\quad - \frac{(1-\gamma)B_0 N t_p E^2}{(N-1)K^2}. \end{aligned} \quad (37)$$

When  $\gamma = 1$ ,  $\frac{\partial \tilde{\mathbb{E}}[C_{\text{tot}}]}{\partial K}$  is always positive, thus,  $K^* = 1$ . However, when  $0 \leq \gamma < 1$ ,  $\frac{\partial \tilde{\mathbb{E}}[C_{\text{tot}}]}{\partial K}$  is negative for small  $K$  and positive for large  $K$ . Thus, as  $K$  increases,  $\tilde{\mathbb{E}}[C_{\text{tot}}]$  first decreases and then increases, thus  $K^* \in [1, N]$ . By letting  $\frac{\partial \tilde{\mathbb{E}}[C_{\text{tot}}]}{\partial K} = 0$ , and dividing  $(1-\gamma)$ , we concludes that  $K^*$  decreases as  $\gamma$  due to the fact that  $\frac{\gamma}{(1-\gamma)}$  is an increasing function in  $\gamma$ .

#### APPENDIX D PROOF OF THEOREM 4

Following the proof in Appendix C, we let  $\frac{\partial \tilde{\mathbb{E}}[C_{\text{tot}}]}{\partial K} = 0$ . Then, it is straightforward to obtain that, for any given  $E$  and  $0 < \gamma < 1$ , the optimal  $K$  increases in  $t_p$  while decreases in  $t_m$ ,  $e_m$ , and  $e_p$ . In particular, according to Theorem 3, when  $\gamma = 1$ ,  $K^* = 1$  and thus is independent with  $e_m$  and  $e_p$ .

#### APPENDIX E PROOF OF THEOREM 5

Taking the first order derivative of  $\tilde{\mathbb{E}}[C_{\text{tot}}]$  over  $E$  for any given  $K$ , we have

$$\begin{aligned} \frac{\partial \tilde{\mathbb{E}}[C_{\text{tot}}]}{\partial E} &= B_0 [(1-\gamma)(2t_p E + t_m K) + \gamma K(2e_p E + e_m)] \\ &\quad \cdot \left( 1 + \frac{N-K}{K(N-1)} \right) - \frac{A_0 K [(1-\gamma)t_m + \gamma e_m]}{E^2}. \end{aligned} \quad (38)$$

For any  $0 \leq \gamma \leq 1$ , and any feasible  $K$ , (38) is negative when  $E$  is small and positive when  $E$  is large. Thus, as  $E$  increases,  $\tilde{\mathbb{E}}[C_{\text{tot}}]$  first decreases and then increases.

APPENDIX F  
PROOF OF THEOREM 6

Following the proof in Appendix E, we let  $\frac{\partial \tilde{E}[C_{\text{tot}}]}{\partial E} = 0$ . Then, we have

$$\frac{[(1-\gamma)(2t_p E^3 + t_m K E^2) + \gamma K(2e_p E^3 + e_m E^2)]}{K[(1-\gamma)t_m + \gamma e_m]} = \frac{A_0}{B_0 \left(1 + \frac{N-K}{K(N-1)}\right)}. \quad (39)$$

Thus, it is straightforward to see that the solution of  $E$  increases as  $t_p$  or  $e_p$  decreases.

In particular, when  $\gamma = 0$ , the solution of  $E$  increases in  $\frac{t_m}{t_p}$ . Similarly, when  $\gamma = 1$ , the solution of  $E$  increases in  $\frac{e_m}{e_p}$ .

REFERENCES

- [1] B. Luo, X. Li, S. Wang, J. Huang, and L. Tassiulas, "Cost-effective federated learning design," in *IEEE Conference on Computer Communications (INFOCOM)*, 2021.
- [2] M. Chiang and T. Zhang, "Fog and iot: An overview of research opportunities," *IEEE Internet of Things Journal*, vol. 3, no. 6, pp. 854–864, 2016.
- [3] S. Shalev-Shwartz and S. Ben-David, *Understanding machine learning: From theory to algorithms*. Cambridge university press, 2014.
- [4] Y. Mao, C. You, J. Zhang, K. Huang, and K. B. Letaief, "A survey on mobile edge computing: The communication perspective," *IEEE Communications Surveys & Tutorials*, vol. 19, no. 4, pp. 2322–2358, 2017.
- [5] J. Park, S. Samarakoon, M. Bennis, and M. Debbah, "Wireless network intelligence at the edge," *Proceedings of the IEEE*, vol. 107, no. 11, pp. 2204–2239, 2019.
- [6] P. Kairouz, H. B. McMahan, B. Avent, A. Bellet, M. Bennis, A. N. Bhagoji, K. Bonawitz, Z. Charles, G. Cormode, R. Cummings *et al.*, "Advances and open problems in federated learning," *arXiv preprint arXiv:1912.04977*, 2019.
- [7] B. McMahan, E. Moore, D. Ramage, S. Hampson, and B. A. y Arcas, "Communication-efficient learning of deep networks from decentralized data," in *Artificial Intelligence and Statistics*, 2017, pp. 1273–1282.
- [8] Y. Jiang, S. Wang, V. Valls, B. J. Ko, W.-H. Lee, K. K. Leung, and L. Tassiulas, "Model pruning enables efficient federated learning on edge devices," in *Workshop on Scalability, Privacy, and Security in Federated Learning (SpicyFL) in Conjunction with NeurIPS*, 2020.
- [9] K. Bonawitz, H. Eichner, W. Grieskamp, D. Huba, A. Ingerman, V. Ivanov, C. Kiddon, J. Konečný, S. Mazzocchi, H. B. McMahan *et al.*, "Towards federated learning at scale: System design," in *Systems and Machine Learning (SysML) Conference*, 2019.
- [10] X. Li, K. Huang, W. Yang, S. Wang, and Z. Zhang, "On the convergence of fedavg on non-iid data," in *International Conference on Learning Representations (ICLR)*, 2019.
- [11] H. Yang, H. He, W. Zhang, and X. Cao, "Fedsteg: A federated transfer learning framework for secure image steganalysis," *IEEE Transactions on Network Science and Engineering*, vol. 8, no. 2, pp. 1084–1094, 2021.
- [12] Y. Gao, L. Liu, B. Hu, T. Lei, and H. Ma, "Federated region-learning for environment sensing in edge computing system," *IEEE Transactions on Network Science and Engineering*, vol. 7, no. 4, pp. 2192–2204, 2020.
- [13] N. H. Tran, W. Bao, A. Zomaya, N. M. NH, and C. S. Hong, "Federated learning over wireless networks: Optimization model design and analysis," in *IEEE Conference on Computer Communications (INFOCOM)*, 2019, pp. 1387–1395.
- [14] S. Wang, T. Tuor, T. Salonidis, K. K. Leung, C. Makaya, T. He, and K. Chan, "Adaptive federated learning in resource constrained edge computing systems," *IEEE Journal on Selected Areas in Communications*, vol. 37, no. 6, pp. 1205–1221, 2019.
- [15] J. Wang and G. Joshi, "Adaptive communication strategies to achieve the best error-runtime trade-off in local-update SGD," in *Systems and Machine Learning (SysML) Conference*, 2019.
- [16] H. Yu, S. Yang, and S. Zhu, "Parallel restarted SGD for non-convex optimization with faster convergence and less communication," in *AAAI Conference on Artificial Intelligence*, 2019.
- [17] S. U. Stich, "Local SGD converges fast and communicates little," in *International Conference on Learning Representations (ICLR)*, 2018.
- [18] J. Wang and G. Joshi, "Cooperative SGD: A unified framework for the design and analysis of communication-efficient SGD algorithms," in *ICML Workshop on Coding Theory for Machine Learning*, 2019.
- [19] A. Khaled, K. Mishchenko, and P. Richtárik, "First analysis of local GD on heterogeneous data," *arXiv preprint arXiv:1909.04715*, 2019.
- [20] V. Smith, C.-K. Chiang, M. Sanjabi, and A. S. Talwalkar, "Federated multi-task learning," in *Advances in Neural Information Processing Systems (NeurIPS)*, 2017, pp. 4424–4434.
- [21] T. Li, A. K. Sahu, M. Zaheer, M. Sanjabi, A. Talwalkar, and V. Smith, "Federated optimization in heterogeneous networks," in *Machine Learning and Systems (MLSys) Conference*, 2020.
- [22] W. Liu, L. Chen, Y. Chen, and W. Zhang, "Accelerating federated learning via momentum gradient descent," *IEEE Transactions on Parallel and Distributed Systems*, vol. 31, no. 8, pp. 1754–1766, 2020.
- [23] S. P. Karimireddy, S. Kale, M. Mohri, S. Reddi, S. Stich, and A. T. Suresh, "Scaffold: Stochastic controlled averaging for federated learning," in *International Conference on Machine Learning*. PMLR, 2020, pp. 5132–5143.
- [24] X. Liang, S. Shen, J. Liu, Z. Pan, E. Chen, and Y. Cheng, "Variance reduced local sgd with lower communication complexity," *arXiv preprint arXiv:1912.12844*, 2019.
- [25] M. P. Ranjit, G. Ganapathy, K. Sridhar, and V. Arumugham, "Efficient deep learning hyperparameter tuning using cloud infrastructure: Intelligent distributed hyperparameter tuning with bayesian optimization in the cloud," in *2019 IEEE 12th International Conference on Cloud Computing (CLOUD)*, 2019, pp. 520–522.
- [26] S. Reddi, Z. Charles, M. Zaheer, Z. Garrett, K. Rush, J. Konečný, S. Kumar, and H. B. McMahan, "Adaptive federated optimization," *arXiv preprint arXiv:2003.00295*, 2020.
- [27] M. Chen, H. V. Poor, W. Saad, and S. Cui, "Convergence time optimization for federated learning over wireless networks," *arXiv preprint arXiv:2001.07845*, 2020.
- [28] H. T. Nguyen, V. Schwag, S. Hosseinipour, C. G. Brinton, M. Chiang, and H. V. Poor, "Fast-convergent federated learning," *IEEE Journal on Selected Areas in Communications*, 2020.
- [29] T. Nishio and R. Yonetani, "Client selection for federated learning with heterogeneous resources in mobile edge," in *IEEE International Conference on Communications (ICC)*, 2019, pp. 1–7.
- [30] W. Shi, S. Zhou, and Z. Niu, "Device scheduling with fast convergence for wireless federated learning," in *IEEE International Conference on Communications (ICC)*, 2020, pp. 1–6.
- [31] M. M. Wadu, S. Samarakoon, and M. Bennis, "Federated learning under channel uncertainty: Joint client scheduling and resource allocation," *arXiv preprint arXiv:2002.00802*, 2020.
- [32] H. Wang, Z. Kaplan, D. Niu, and B. Li, "Optimizing federated learning on non-iid data with reinforcement learning," in *IEEE Conference on Computer Communications (INFOCOM)*, 2020, pp. 1698–1707.
- [33] H. H. Yang, Z. Liu, T. Q. Quek, and H. V. Poor, "Scheduling policies for federated learning in wireless networks," *IEEE Transactions on Communications*, vol. 68, no. 1, pp. 317–333, 2019.
- [34] X. Mo and J. Xu, "Energy-efficient federated edge learning with joint communication and computation design," *arXiv preprint arXiv:2003.00199*, 2020.
- [35] Q. Zeng, Y. Du, K. Huang, and K. K. Leung, "Energy-efficient resource management for federated edge learning with CPU-GPU heterogeneous computing," *arXiv preprint arXiv:2007.07122*, 2020.
- [36] Z. Yang, M. Chen, W. Saad, C. S. Hong, and M. Shikh-Bahaei, "Energy efficient federated learning over wireless communication networks," *arXiv preprint arXiv:1911.02417*, 2019.
- [37] S. Luo, X. Chen, Q. Wu, Z. Zhou, and S. Yu, "Hfel: Joint edge association and resource allocation for cost-efficient hierarchical federated edge learning," *arXiv preprint arXiv:2002.11343*, 2020.
- [38] P. Han, S. Wang, and K. K. Leung, "Adaptive gradient sparsification for efficient federated learning: An online learning approach," in *IEEE International Conference on Distributed Computing Systems (ICDCS)*, 2020.
- [39] W. Luping, W. Wei, and L. Bo, "CMFL: Mitigating communication overhead for federated learning," in *IEEE International Conference on Distributed Computing Systems (ICDCS)*, 2019, pp. 954–964.
- [40] K. Hsieh, A. Harlap, N. Vijaykumar, D. Konomis, G. R. Ganger, P. B. Gibbons, and O. Mutlu, "Gaia: Geo-distributed machine learning approaching LAN speeds," in *USENIX Symposium on Networked Systems Design and Implementation (NSDI)*, 2017, pp. 629–647.

- [41] Y. Jin, L. Jiao, Z. Qian, S. Zhang, S. Lu, and X. Wang, "Resource-efficient and convergence-preserving online participant selection in federated learning," in *IEEE International Conference on Distributed Computing Systems (ICDCS)*, 2020.
- [42] G. Zhu, Y. Wang, and K. Huang, "Broadband analog aggregation for low-latency federated edge learning," *IEEE Transactions on Wireless Communications*, vol. 19, no. 1, pp. 491–506, 2019.
- [43] K. Yang, T. Jiang, Y. Shi, and Z. Ding, "Federated learning via over-the-air computation," *IEEE Transactions on Wireless Communications*, vol. 19, no. 3, pp. 2022–2035, 2020.
- [44] M. M. Amiri and D. Gündüz, "Machine learning at the wireless edge: Distributed stochastic gradient descent over-the-air," *IEEE Transactions on Signal Processing*, vol. 68, pp. 2155–2169, 2020.
- [45] J. Gorski, F. Pfeuffer, and K. Klamroth, "Biconvex sets and optimization with biconvex functions: a survey and extensions," *Mathematical methods of operations research*, vol. 66, no. 3, pp. 373–407, 2007.
- [46] T. Li, A. K. Sahu, A. Talwalkar, and V. Smith, "Federated learning: Challenges, methods, and future directions," *IEEE Signal Processing Magazine*, vol. 37, no. 3, pp. 50–60, 2020.